Available online at www.sciencedirect.com
SCIENCE DIRECT®
Journal of Solid State Chemistry 177 (2004) 262–267
JOURNAL OF SOLID STATE CHEMISTRY
http://elsevier.com/locate/jssc

# A Mössbauer study of oxygen vacancy and cation distribution in 6H-$BaTi_{1-x}Fe_xO_{3-x/2}$

E. Mashkina,[a] C. McCammon,[b,*] and F. Seifert[b]

[a] *Kristallographie und Strukturphysik, Universität Erlangen-Nürnberg, Erlangen D-91054, Germany*
[b] *Bayerisches Geoinstitut, Universität Bayreuth, Bayreuth D-95440, Germany*

Received 5 May 2003; received in revised form 26 July 2003; accepted 7 August 2003

**Abstract**

We have synthesized samples in the system $BaTi_{1-x}Fe_xO_{3-x/2}$ with $x = 0.1 - 0.6$ at temperatures of 1200–1300°C under reducing conditions of oxygen fugacity. After drop quenching, samples were characterized using the electron microprobe, X-ray diffraction and Mössbauer spectroscopy. All samples were hexagonal with a 6H-$BaTiO_3$ type structure. Mössbauer spectroscopy showed all iron to be present as $Fe^{3+}$, occurring in octahedral and pentahedral sites. Analysis of area ratios indicates that oxygen vacancies are distributed randomly over O1 sites, and that a random distribution of Fe and Ti cations over *M*1 and *M*2 sites is consistent with the data. No evidence for ordering of oxygen vacancies was found. Results are consistent with conductivity results, which show generally increasing ionic conductivity with increasing oxygen vacancy concentration.


*Keywords:* Mössbauer spectroscopy; Ionic conductivity; Barium titanate; Ferric iron; Oxygen vacancy; Perovskite

## 1. Introduction

Considerable interest has been focused on the defect structure and transport properties of perovskite-type compounds due to their important technological applications, including uses in electrochemical devices such as fuel cells, gas sensors, and membranes for oxygen extraction or hydrogen production. Their thermal and chemical stability is a decisive advantage in these applications; thus it is important to understand the properties that are relevant to fast oxygen transport. $BaTiO_3$-based ceramics are mixed conductors showing both ionic and electronic conductivities (n- and p-type) at elevated temperatures, where the electrical properties are controlled by doping with aliovalent impurities. One interesting aspect of these compounds is their ability to accommodate anion vacancies in order to maintain electrostatic neutrality when $Ti^{4+}$ is replaced by $Fe^{3+}$. These vacancies lead to high ionic and electronic conductivities, and thus promote better performance as electrochemical devices. In this study we focused on the vacancy structure of $Fe^{3+}$-substituted $BaTiO_3$.

The structure of 6H-$BaTiO_3$ is constructed from six $BaO_3$ layers in cubic (*c*) and hexagonal (*h*) close packing in the sequence *hcchcc* [1] (Fig. 1). Ti2 atoms occupy pairs of face-shared octahedra, while Ti1 atoms are situated in octahedra between *c* layers that share corners with Ti2 octahedra. When $Ti^{4+}$ is substituted by $Fe^{3+}$, oxygen vacancies are created according to the electroneutrality condition $[Fe'_{Ti}] = 2[V_O^{\bullet\bullet}]$, and appear to be confined to the O1 site [2]. Removal of one oxygen atom from the common face shared by adjacent *M*2 sites creates a pair of edge-shared pentahedra (Fig. 1).

There is an extensive solid solution of 6H-$BaTi_{1-x}Fe_xO_{3-\delta}$ that extends to ca. $x = 0.67$, depending on temperature and oxygen fugacity [2,3]. Close to the $BaTiO_3$ end member, $Fe^{3+}$ is stable over a wide range of oxygen partial pressures (from $10^{-4}$ to $10^{-22}$ bar at 700°C) [4], while $Fe^{4+}$ becomes more stable relative to $Fe^{3+}$ under oxidizing conditions as the iron concentration increases [2].

There is limited Mössbauer data for $BaTi_{1-x}Fe_xO_{3-\delta}$. Studies near the $BaTiO_3$ end member focused on the behavior of $Fe^{4+}$, and consequently found it difficult to prepare samples except under highly oxidizing

*Corresponding author. Fax: +49-(0)921-553769.
*E-mail address:* catherine.mccammon@uni-bayreuth.de (C. McCammon).

0022-4596/$ - see front matter © 2003 Elsevier Inc. All rights reserved.
doi:10.1016/j.jssc.2003.08.008

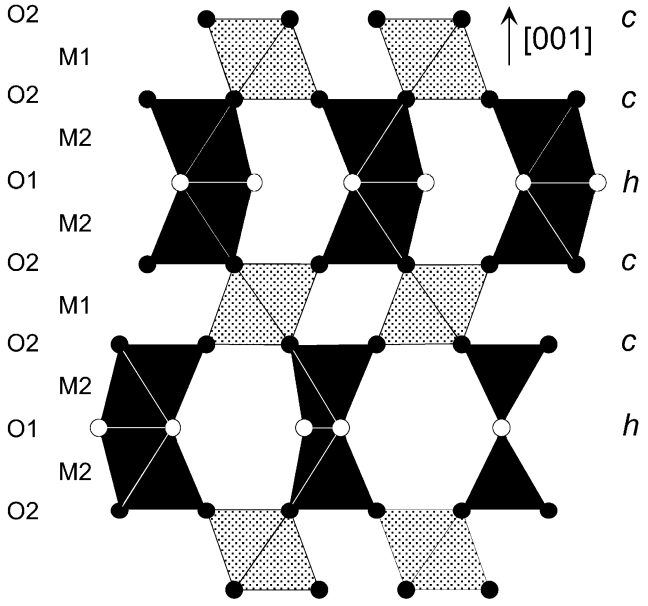


Fig. 1. Crystal structure of 6H-$BaTi_{1-x}Fe_xO_{3-\delta}$ looking down [110]. Structural units are shaded as follows: *M*1 octahedron: light gray; *M*2 octahedron: black; O1 atoms: black; O2 atoms: white. Ba atoms have been omitted for clarity. The bottom row of *M*2 dimers shows the effect of zero, one or two oxygen vacancies associated with the pair (from left): face-shared octahedra, edge-shared pentahedra, and corner-shared tetrahedra, respectively. The sequence of cubic (*c*) and hexagonal (*h*) close packed $BaO_3$ layers are indicated, as well as layers containing O1/O2 atoms and *M*1/*M*2 sites.

conditions [4,5]. $Fe^{4+}$ occurred as a quadrupole doublet at room temperature with narrow line width and center shift (relative to α-Fe) of −0.01 mm/s, while $Fe^{3+}$ could only be resolved as a broad quadrupole doublet with center shift (relative to α-Fe) near 0.3 mm/s [4]. At the other end member, studies of $BaFeO_{2.95}$ reported similar results: a narrow quadrupole doublet assigned to $Fe^{4+}$ at room temperature with center shift (relative to α-Fe) of −0.06 mm/s and a broad quadrupole doublet assigned to $Fe^{3+}$ with center shift (relative to α-Fe) near 0.5 mm/s [6]. None of the studies were able to resolve the $Fe^{3+}$ quadrupole doublet sufficiently to determine $Fe^{3+}$ site distribution.

In this paper we report the first Mössbauer study of $BaTi_{1-x}Fe_xO_{3-x/2}$ samples synthesized over a range of compositions in order to investigate cation distribution and short-range ordering of oxygen vacancies, and discuss potential implications for the interpretation of conductivity data.

## 2. Experimental methods

Polycrystalline samples of $BaTi_{1-x}Fe_xO_{3-\delta}$ ($x = 0.1, 0.2, 0.3, 0.6$) were prepared via solid state reaction at high temperature under controlled atmosphere. Appropriate amounts of reagent-grade $BaCO_3$, $Fe_2O_3$ and $TiO_2$ powders were mixed in an agate mortar under ethanol for about 30 min, and heated in a crucible in air for 37–114 h at temperatures ranging from 1200°C to 1300°C (run times and temperatures decreased with increasing iron concentration). An additional sample of $BaTi_{0.9}Fe_{0.1}O_{3-\delta}$ was prepared using the same methods with a $^{57}Fe$ enrichment of 30%. All run products were analyzed by electron microprobe, and were found to be close to the nominal composition (Table 1). Materials were then heated in open AgPd capsules at temperatures of 1200°C in CO–$CO_2$ gas mixtures corresponding to an oxygen fugacity of $\log f O_2 = -11$. Samples were drop quenched into a cool part of the furnace under flowing gas and examined using X-ray diffraction and Mössbauer spectroscopy.

X-ray intensity data were collected on a Siemens D-5000 diffractometer using Cu*K*α radiation. Step scan intensity measurements were made in the 2θ range 20–80° at intervals of 0.02°. All samples were found to be single phase. The crystal structure of $BaTi_{1-x}Fe_xO_{3-x/2}$ ($x = 0.1 - 0.6$) was determined to be hexagonal with 6H-$BaTiO_3$ type, where the variation of unit cell parameters is consistent with previous results in the literature [3].

Samples for Mössbauer spectroscopy were prepared by mixing powdered materials with benzophenone and mounting in Plexiglass sample holders. Sample weights were calculated to provide the optimum sample thickness while minimizing thickness effects [7], and varied from 1 to 5 mg Fe/$cm^2$. Mössbauer spectra were recorded at room temperature (293 K) in transmission mode on a constant acceleration Mössbauer spectrometer with a nominal 1.85 GBq $^{57}Co$ source in a 6 μm Rh matrix. Spectra took typically 3 days each to collect. The velocity scale was calibrated relative to 25 μm α-Fe foil using the positions certified for National Bureau of Standards standard reference material no. 1541; line widths of 0.28 mm/s for the outer lines of α-Fe were obtained at room temperature. The spectra were fitted to Lorentzian lineshapes using the commercially available fitting program NORMOS written by R.A. Brand (distributed by Wissenschaftliche Elektronik GmbH, Germany).

## 3. Results

The Mössbauer spectra of $BaTi_{1-x}Fe_xO_{3-x/2}$ consist of multiple overlapping doublets (Fig. 2). The fitting approach took into account the structure of 6H-$BaTi_{1-x}Fe_xO_{3-x/2}$, and the range of center shifts observed for octahedral and pentahedral $Fe^{3+}$ in $CaTi_{1-x}Fe_xO_{3-x/2}$ [8]. The validity of fits was judged on the basis of minimizing the number of parameters and $\chi^2$ values, providing physically realistic fits to the spectra, and achieving consistency across the

Table 1
Hyperfine parameters for $BaTi_{1-x}Fe_xO_{3-x/2}$ at 293 K

| Fe concentration ($x$) | 0.1[a] | 0.12(3) | 0.20(2) | 0.31(5) | 0.62(5) |
|---|---|---|---|---|---|
| *$^{VI}Fe^{3+}$ doublet* | | | | | |
| CS (mm/s) | *0.33* | *0.33* | 0.33(1) | 0.34(1) | 0.34(2) |
| QS (mm/s) | 0.32(2) | 0.43(8) | 0.35(3) | 0.38(2) | 0.33(2) |
| $\Gamma$ (mm/s) | 0.41(4) | 0.24(17) | 0.28(6) | 0.30(6) | 0.40(4) |
| Area (%) | 35(20) | 13(20) | 33(13) | 37(21) | 39(8) |
| *$^{VI}Fe^{3+}$ singlet* | | | | | |
| CS (mm/s) | *0.32* | *0.32* | 0.32(1) | 0.33(1) | |
| $\Gamma$ (mm/s) | *0.40* | 0.38(18) | 0.27(8) | 0.25(20) | |
| Area (%) | 16(20) | 34(28) | 18(9) | 8(8) | |
| *$^{V}Fe^{3+}$(I) doublet* | | | | | |
| CS (mm/s) | 0.29(2) | 0.26(3) | 0.27(1) | 0.26(1) | 0.25(1) |
| QS (mm/s) | 0.67(2) | 0.68(3) | 0.71(2) | 0.73(2) | 0.73(6) |
| $\Gamma$ (mm/s) | *0.50* | 0.45(7) | 0.37(2) | 0.38(2) | 0.37(9) |
| Area (%) | 49(20) | 53(16) | 49(5) | 55(5) | 44(10) |
| *$^{V}Fe^{3+}$(II) doublet* | | | | | |
| CS (mm/s) | | | | | 0.25(1) |
| QS (mm/s) | | | | | 1.06(10) |
| $\Gamma$ (mm/s) | | | | | 0.32(12) |
| Area (%) | | | | | 17(10) |
| $^{V}Fe^{3+}$ (cations per formula unit) | 0.05(2) | 0.06(2) | 0.10(1) | 0.17 (2) | 0.38(9) |
| $^{VI}Fe^{3+}$ (cations per formula unit) | 0.05(2) | 0.06(2) | 0.10(1) | 0.14 (2) | 0.24(5) |

*Note*: CS: center shift (relative to α-Fe); QS: quadrupole splitting; $\Gamma$: Lorentzian line width; area: relative area.
Values in italics were held fixed during the fitting process.
[a] Nominal composition; synthesized with $^{57}Fe$.

composition range. Conventional constraints were applied to the high- and low-velocity components of each doublet (i.e. equal area and equal width). The final fitting model consists of one singlet assigned to octahedral $Fe^{3+}$, one doublet assigned to octahedral $Fe^{3+}$, and two doublets assigned to pentahedral $Fe^{3+}$. Hyperfine parameters are listed in Table 1, where uncertainties are estimated based on statistical errors of the particular fitting model, as well as uncertainties in the model itself. Caution must be exercised in spectral interpretation due to the overlap of spectral components; hence in the following discussion, we focus primarily on the parameters that are well constrained by the data, namely the center shifts and the proportion of pentahedral $Fe^{3+}$ absorption relative to total absorption.

The presence of $Fe^{2+}$ was ruled out based on the absence of absorption at higher velocity (a center shift of at least 1.0 mm/s relative to α-Fe would be expected, e.g. [9]) and the presence of $Fe^{4+}$ was ruled out based on the weighted mean center shifts (a parameter which is relatively independent of the fitting model) which all fall within the range for $Fe^{3+}$. The absence of $Fe^{4+}$ is consistent with previous work and the relatively reducing conditions used to synthesize the samples.

A minimum of two subspectra are required to fit octahedral $Fe^{3+}$ absorption in Mössbauer spectra of 6H-$BaTi_{1-x}Fe_xO_{3-x/2}$, likely reflecting a distribution of $Fe^{3+}$ between the $M1$ and $M2$ sites. Most fitting trials with two octahedral $Fe^{3+}$ doublets of spectra from samples with low iron concentration returned zero for the quadrupole splitting of one of the doublets, hence we modeled octahedral $Fe^{3+}$ absorption as one doublet and one singlet. At low iron concentrations the singlet could be interpreted to indicate $Fe^{3+}$ in the $M1$ site (since it has cubic symmetry the quadrupole splitting should be zero), but the absence of the singlet in spectra from higher iron concentrations does not exclude the possibility of $Fe^{3+}$ occupying the $M1$ site. Symmetry could be lowered in the $M1$ site at higher iron concentrations (e.g. by next-nearest neighbor interactions) such that quadrupole splitting is no longer zero.

Hyperfine parameters for pentahedral $Fe^{3+}$ in $BaTi_{1-x}Fe_xO_{3-x/2}$ are similar to those for pentahedral $Fe^{3+}$ in $CaTi_{1-x}Fe_xO_{3-x/2}$ [8]. One doublet was sufficient to model absorption assigned to pentahedral $Fe^{3+}$ in all $BaTi_{1-x}Fe_xO_{3-x/2}$ spectra except for $x = 0.6$, where an additional doublet was required. In all fitting trials the center shift of the two doublets in the $x = 0.6$ spectrum assigned to pentahedral $Fe^{3+}$ were identical within experimental error, suggesting that the second doublet might correspond to a slightly different next-nearest neighbor environment. Such a difference could arise between pentahedral dimers occupied by Ti and

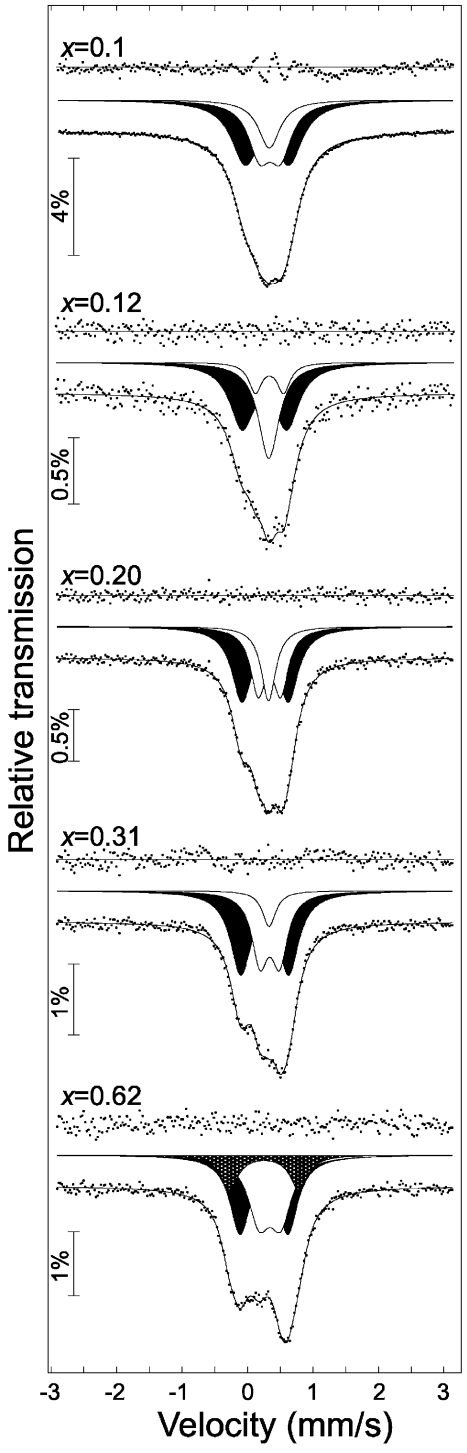


Fig. 2. Room temperature Mössbauer spectra of $BaTi_{1-x}Fe_xO_{3-x/2}$ quenched from 1200°C and log $fO_2 = -11$ corresponding to the indicated compositions. The top spectrum corresponds to a sample 30% enriched in $^{57}Fe$, while all others correspond to unenriched samples. Subspectra are shaded as follows: singlet and doublet octahedral $Fe^{3+}$ (white); doublet pentahedral $Fe^{3+}$ (black); second doublet pentahedral $Fe^{3+}$ (dark gray). Note the limited resolution for determining the individual contributions to octahedral $Fe^{3+}$ absorption—although the relative areas for singlet and doublet octahedral $Fe^{3+}$ vary significantly in the top two spectra, the shape of the overall spectral envelopes is basically the same.

$Fe^{3+}$, compared to those where $Fe^{3+}$ occupies both sites of the dimer. We consider it unlikely that the additional doublet could correspond to tetrahedral $Fe^{3+}$, since a significant difference in center shift (greater than at least 0.02 mm/s) would be expected on removal of a coordinating oxygen.

## 4. Discussion

In Mössbauer spectroscopy, the relative area of a subspectrum is related to the relative abundance of iron on the corresponding crystallographic site, and to a first approximation the two can be considered equal. The relative area fractions can therefore be used to calculate the relative abundance of $Fe^{3+}$ in the octahedral and pentahedral sites, and show that the number of Fe atoms on pentahedral sites is approximately equal to the number of Fe atoms on octahedral sites up to iron concentrations of $x = 0.2$ (Table 1).

For samples of $BaTi_{1-x}Fe_xO_{3-x/2}$ containing only $Fe^{3+}$, and assuming that all Ti is present as $Ti^{4+}$, the number of oxygen vacancies can be calculated directly from the iron concentration based on electrostatic neutrality. Fig. 3 shows a comparison of this value with the one calculated from the Mössbauer data, based on one half oxygen vacancy per pentahedral site. The 1:1

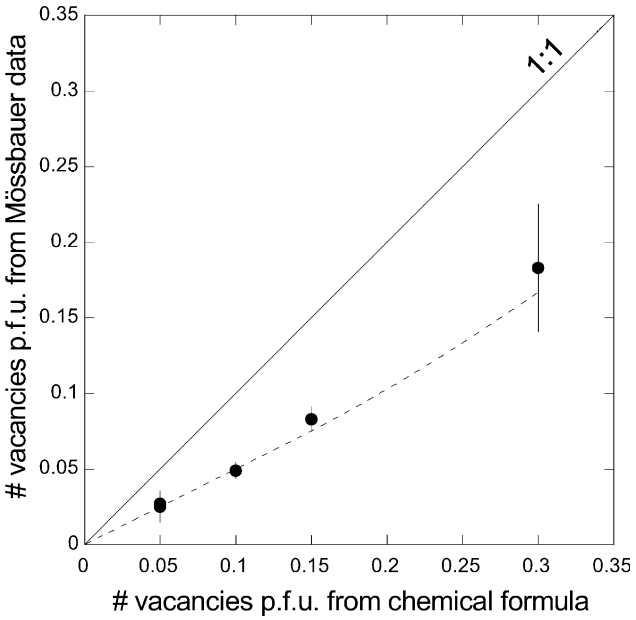


Fig. 3. Site distribution of pentahedral sites in $BaTi_{1-x}Fe_xO_{3-x/2}$ quenched from 1200°C and log $fO_2 = -11$. Data points represent the number of $Fe^{3+}$ cations occupying pentahedral sites per formula unit (p.f.u.) as determined from the Mössbauer data, where the difference between data points and the 1:1 correlation gives the number of $Ti^{4+}$ cations on pentahedral sites. The dotted line indicates the trend that would be predicted for the Mössbauer data if $Ti^{4+}$ and $Fe^{3+}$ were distributed equally over all cation sites.

correlation line indicates the variation expected if oxygen vacancies were only associated with Fe atoms. In this case each oxygen vacancy would be associated with two Fe atoms occupying both sites of an $M2$–$M2$ pair, and no Fe would substitute onto the $M1$ site. We can rule out this possibility based on the systematic offset of the data from this line in Fig. 3, and the degree to which the data deviate from the 1:1 correlation indicates the number of Ti atoms that are associated with oxygen vacancies.

We can calculate the number of oxygen vacancies associated with Fe and Ti based on a random distribution of cations over available sites. For samples with $x<0.5$, half of the pentahedral sites would be occupied by $Fe^{3+}$ and half would be occupied by $Ti^{4+}$. $M2$ dimers containing an oxygen vacancy are considered more likely to be Fe–Ti, rather than Ti–Ti or Fe–Fe. At higher iron concentrations, however, there are insufficient Ti atoms available to balance Fe; hence Fe–Fe pairs on the $M2$ site would become more common. This variation is indicated by the dotted line in Fig. 3, where Fe is associated with 50% of the pentahedral sites up to $x=0.5$, but an increasing fraction at higher iron concentrations. The dotted line appears to fit our Mössbauer data well, indicating that a random distribution of oxygen vacancies over O1 sites is consistent with our data.

The actual distribution of Fe and Ti over $M1$ and $M2$ cation sites is more difficult to determine. In principle the site distribution could be determined from the relative area data, but since the singlet and doublet assigned to octahedral $Fe^{3+}$ absorption overlap significantly, the errors would be extremely large. There is a possibility, however, to use the relative areas of pentahedral and octahedral subspectra to infer some qualitative aspects of the cation distribution over $M1$ and $M2$ sites. We consider two different cases where oxygen vacancies are randomly distributed over O1 sites as described above: (1) Fe and Ti are randomly distributed over $M1$ and $M2$ sites (dotted line in Fig. 3); and (2) Fe substitutes on the $M2$ site only. At low iron concentrations, both cases would give a similar ratio for pentahedral to octahedral sites, since oxygen vacancies are also low in concentration. At higher iron concentrations, however, the chance of Fe–Fe pairs is significantly greater when Fe substitutes on the $M2$ site only, so that more oxygen vacancies are associated with Fe atoms. For an iron concentration of $x=0.6$, for example, the number of oxygen vacancies associated with Fe atoms for case (2) would be 0.27 per formula unit (p.f.u.), compared to 0.17 p.f.u. for case (1). It is clear that the latter value is more consistent with the Mössbauer data (Fig. 3), and so we conclude that Fe *does* substitute on the $M1$ site, and that a random distribution of Fe and Ti atoms over the $M1$ and $M2$ sites is at least consistent with our data.

Our Mössbauer data do not support the presence of tetrahedral $Fe^{3+}$. This is in contrast to the results inferred from Rietveld refinements of 6H-$BaTi_{0.33}Fe_{0.67}O_{3-\delta}$ synthesized at significantly higher oxygen fugacities (in air and in flowing oxygen) [10]. A portion of iron in the high vacancy sample ($\delta\sim0.32$ based on weight loss) was inferred to be tetrahedrally coordinated based on differences in the $z$ positional parameter for the $M2$ site between neutron and X-ray data, where Fe and Ti could be distinguished in neutron data due to the opposite signs of their neutron scattering lengths. Comparison of these results with the present Mössbauer data suggests that the coordination of $Fe^{3+}$ (and hence the nature of oxygen vacancy ordering) may depend on $Fe^{4+}/Fe^{3+}$, since we observed that samples with similar iron concentration synthesized in air always contained observable $Fe^{4+}$ (typically $\frac{1}{3}$ of Fe) according to Mössbauer spectroscopy.

The distribution of oxygen vacancies in $BaTi_{1-x}Fe_xO_{3-\delta}$ provides insight into its conductivity. Ionic conductivity has been observed for samples in the concentration range $x=0.1$ to 0.5 [11], although the magnitude is significantly less for equivalent compositions and temperatures compared to $CaTi_{1-x}Fe_xO_{3-\delta}$ [12] and $SrTi_{1-x}Fe_xO_{3-\delta}$ [13]. One possible factor is a reduced mobility of oxygen ions in $BaTi_{1-x}Fe_xO_{3-\delta}$, since oxygen vacancies are essentially constrained to two-dimensional movement along planes of O1 atoms. In contrast, oxygen vacancies can move in three dimensions at low iron concentrations within perovskite-structured $SrTi_{1-x}Fe_xO_{3-\delta}$ and $CaTi_{1-x}Fe_xO_{3-\delta}$, e.g. [8]. On the other hand, ionic conductivity generally increases with increasing vacancy concentration in $SrTi_{1-x}Fe_xO_{3-\delta}$ and $BaTi_{1-x}Fe_xO_{3-\delta}$, but decreases in $CaTi_{1-x}Fe_xO_{3-\delta}$ after reaching a maximum near $x=0.2$ [12]. This can be attributed to the ordering of oxygen vacancies in $CaTi_{1-x}Fe_xO_{3-\delta}$ into chains and eventually infinite planes, which dramatically reduces the mobility of vacancies [8]. In contrast, the lack of vacancy ordering in $SrTi_{1-x}Fe_xO_{3-\delta}$ ($x<0.8$) and $BaTi_{1-x}Fe_xO_{3-\delta}$ leads to an enhancement of ionic conductivity with increasing concentration of oxygen vacancies. The presence of tetrahedral $Fe^{3+}$ in $BaTi_{1-x}Fe_xO_{3-\delta}$ [10], which implies short-range ordering of vacancies within planes of O1 atoms, would restrict the mobility of ionic charge carriers. There may be conditions, therefore, under which ionic conductivity is favored compared to others, and a combined study incorporating Mössbauer spectroscopy and conductivity measurements could help to identify those conditions.

## Acknowledgments

A. Magerl and M. Goebbels contributed support and helpful discussions to the project, while F. Gaillard

assisted with synthesis experiments involving the gas-flow furnace. Funding for a Ph.D. student fellowship (E.M.) was provided by the Deutsche Forschungsgemeinschaft (Germany).

## References

[1] J. Akimoto, Y. Gotoh, Y. Oosawa, Acta Crystallogr. C 50 (1994) 160–161.
[2] I.E. Grey, C. Li, L.M.D. Cranswick, R.S. Roth, T.A. Vanderah, J. Solid State Chem. 135 (1998) 312–321.
[3] T.A. Vanderah, J.M. Loezos, R.S. Roth, J. Solid State Chem. 121 (1996) 38–50.
[4] A. Hero, U. Gonser, H. Engelmann, H.J. Hagemann, Ferroelectrics 65 (1985) 211–216.
[5] W. Wildner, U. Gonser, H. Schmitt, J. Albers, S.K. Date, Ferroelectrics 23 (1980) 193–198.
[6] P.K. Gallagher, J.B. MacChesney, D.N.E. Buchanan, J. Chem. Phys. 43 (1965) 516–520.
[7] G.L. Long, T.E. Cranshaw, G. Longworth, Möss. Effect Ref. Data J. 6 (1983) 42–49.
[8] C.A. McCammon, A.I. Becerro, F. Langenhorst, R. Angel, S. Marion, F. Seifert, J. Phys.: Condens. Matt. 12 (2000) 2969–2984.
[9] C.A. McCammon, in: S. Redfern, M. Carpenter (Eds.), Transformation Processes in Minerals, Mineralogical Society of America, Washington, DC, 2000, pp. 241–264.
[10] I.E. Grey, L.M.D. Cranswick, C. Li, J. Appl. Crystallogr. 31 (1998) 692–699.
[11] E.A. Mashkina, L.A. Dunuyshkina, A.K. Demin, M. Göbbels, R. Hock, A. Magerl, in: J. Huijsmans (Ed.), Fifth European Solid Oxide Fuel Cell Forum Proceedings, Vol. 2, European Fuel Cell Forum, Switzerland, 2002, pp. 695–699.
[12] S. Marion, A.I. Becerro, T. Norby, Ionics 5 and 6 (1999) 385–392.
[13] S. Steinsvik, T. Norby, P. Kofstad, in: R. Waser, S. Hoffman, D. Bonnenberg, C. Hoffman (Eds.), Proceedings Electroceramics IV, Fourth International Conference on Electroceramics and Applications, Augustinus Buchhandlung, Aachen, 1994, pp. 691–696.